*Laser and Particle Beams*

**cambridge.org/lpb**

# Temporal measurements of extreme ultraviolet (EUV) emission, from low temperature, EUV-induced plasmas

A. Bartnik, H. Fiedorowicz, P. Wachulak and T. Fok

Institute of Optoelectronics, Military University of Technology, Warsaw, Poland

**Research Article**

**Cite this article:** Bartnik A, Fiedorowicz H, Wachulak P, Fok T (2018). Temporal measurements of extreme ultraviolet (EUV) emission, from low temperature, EUV-induced plasmas. *Laser and Particle Beams* **36**, 286–292. https://doi.org/10.1017/S0263034618000319

Received: 6 June 2018
Accepted: 24 July 2018

**Key words:**
EUV detectors; EUV optics; EUV source; laser-produced plasma

**Author for correspondence:**
A. Bartnik, Institute of Optoelectronics, Military University of Technology, Warsaw, Poland.
E-mail: andrzej.bartnik@wat.edu.pl

**Abstract**

In this work, extreme ultraviolet (EUV) emission, from EUV induced, low-temperature microplasmas, were investigated. To perform temporal measurements of the EUV pulses of low intensity, in a medium vacuum, under the pressure of the order of 0.1–0.01 mbar a special detection system was prepared. The system was based on an EUV collector and a semiconductor detector, sensitive for the EUV photons. The collector consisted of two identical grazing incidence, paraboloidal mirrors, and allowed to focus a part of the radiation emitted from the microplasma onto the detector surface. An absorption filter, mounted between the collector and the detector, allowed for selection of an interesting wavelength range. Plasmas were created by irradiation of small portions of gases, injected into the vacuum chamber, using a laser produced plasma EUV source. Three gases were used for the EUV induced plasma formation: neon, krypton, and xenon. Low-temperature plasmas, created in these gases, contained multiply charged ions, emitting radiation in similar wavelength ranges. Two detectors, AXUV20HS1 and AXUVHS5, were used for the measurements. It was shown that differences between the corresponding signal profiles, obtained using both detectors, were not very significant. Moreover, it was demonstrated that the duration of the EUV emission from plasmas, created in different gases, were comparable with the duration of the driving EUV pulse. The longest EUV emission was observed for Kr plasmas, approximately 1.5 times the full width half maximum of the driving EUV pulse.

## Introduction

Many measurement instruments and methods were developed for the detection of electromagnetic radiation from different spectral ranges. From obvious reasons different kinds of detection systems for visible light, ultraviolet (UV) or even X-ray ranges are in a common use. There are, however, spectral ranges like extreme UV (EUV) or soft X-rays (SXR), important mainly for science or advanced emerging technologies, for which specialized detection systems have to be prepared. It concerns especially extremely high or weak radiation signals. In many cases, there are no commercially available instruments for measurements of the radiation parameters in such conditions. In case of measurements of the radiation beams with an extremely high intensity, only some indirect methods can be employed and these methods are still under development Gerasimova *et al.* (2013), Chalupský *et al.* (2015). It concerns especially free electron lasers, with the brilliance of several orders of magnitude higher compared with synchrotrons or other EUV sources Huang (2013). On the other hand, EUV induced fluorescence in the EUV range Bartnik *et al.* (2008) gives signals with intensity several orders of magnitude lower comparing to the driving radiation. Such signals can be measured employing multichannel plate (MCP) amplifiers Könneckea *et al.* (2013), Bartnik *et al.* (2015). Although MCPs offer the possibility to detect extremely weak signals with spatial and temporal resolution, hence, are employed for time-resolved imaging or spectral measurements, their use has some significant limitations. One of them is connected with a presence of a strong electric field, necessary for proper operation of MCPs. For this reason, MCPs can be used only in the high vacuum environment. In many cases this is not a problem because the EUV radiation propagates only in a vacuum, so the measurements have to be performed in the vacuum chamber. In some cases, however, the vacuum cannot be maintained at a sufficiently high level for the MCP operation and in these cases, some other detection system has to be applied. Such situation exists, for example, in technological systems designed for EUV lithography, where the high vacuum cannot be maintained due to plasma production with high repetition rate and presence of mitigation systems based on hydrogen or other gases Abrikosov *et al.* (2017), van der Horst *et al.* (2016). In case of scientific research poor vacuum is encountered, for example, in experiments concerning the interaction of the EUV radiation with gaseous media. This kind of investigations is conducted for many years by the authors of this paper using laser plasma EUV sources developed by themselves. Of course, MCP-based systems



CAMBRIDGE UNIVERSITY PRESS

can be employed even in case of poor vacuum. In this case, however, a differential pumping system is necessary, which significantly complicates the vacuum system.

In this work, a detection system capable to measure weak EUV signals with a temporal resolution was prepared. In this system, instead of using the MCP for the EUV detection, semiconductor EUV sensitive photodiodes are employed. To increase the photon flux reaching the detector active area, a specially prepared EUV collector, based on paraboloidal mirrors, was used. In contrary to MCPs, such a system can work in a poor vacuum. The only limitation is the EUV absorption in the residual gas. In most cases the vacuum at a level of 0.1–0.01 mbar is sufficient. The source of weak EUV signals is a low-temperature plasma, created by EUV photoionization of a small portion of gas injected into a vacuum chamber. Measurements of time profiles of the EUV pulses, emitted from such microplasmas, using the detection system were performed.

## Experimental arrangement

An experimental arrangement consists of two basic systems: a laser produced plasma (LPP) SXR/EUV radiation source and a system for the creation and investigation of EUV induced low-temperature plasmas. The first one produces intense radiation pulses that can be used for various experiments concerning EUV or SXR interaction with matter. The second one allows for measurements of the EUV radiation pulses of low intensity, emitted from plasmas driven by the LPP source. A schematic view of the experimental arrangement is presented in Figure 1.

### *The LPP SXR/EUV source*

The LPP source is based on a 10-Hz Nd:YAG laser system (NL 129, EKSPLA) and a double-stream gas-puff target. The NL 129 system can deliver laser pulses with energy up to 10 J at a wavelength of 1.06 μm. Two options concerning the pulse length are possible: long $\tau \approx 10$ ns and the short pulse regime $\tau \approx 1$ ns. The gaseous target was formed by pulsed injection of a xenon gas into a hollow stream of helium (Xe/He target) by employing an electromagnetic valve system, equipped with a double nozzle set-up. The laser beam was focused on the target allowing to create Xe plasmas emitting intense radiation in the EUV ($\tau \approx 10$ ns) or SXR ($\tau \approx 1$ ns) spectral range. Typical spectra of the emitted radiation in both wavelength ranges are presented in Figure 2. The SXR spectrum (Fig. 2a) contains three distinct features, composed of a large number of partially overlapping lines in the wavelength range 1 ÷ 2 nm and long-wavelength tail ranging up to approximately 7 nm.

The EUV spectrum (Fig. 2b) spans a wide wavelength range with the most intense emission between 3 and 16 nm with a maximum at the wavelength of approximately 11 nm. Both spectra were obtained using a home-made spectrograph based on a 5000 l/mm free-standing transmission grating. The EUV radiation was focused using a gold-plated grazing incidence ellipsoidal collector, manufactured by RITE s.r.o., Czech Republic. The collector allowed for effective focusing of the radiation in the wavelength range $\lambda \geq 9$ nm. Hence, the radiation corresponding to the most intense part of the spectrum could be collected in a focal spot. The EUV fluence in a focal plane of the collector reached 0.4 J/cm$^2$ at the center of the focal spot. An FWHM of the intensity distribution across the focal spot was approximately 1.4 mm.

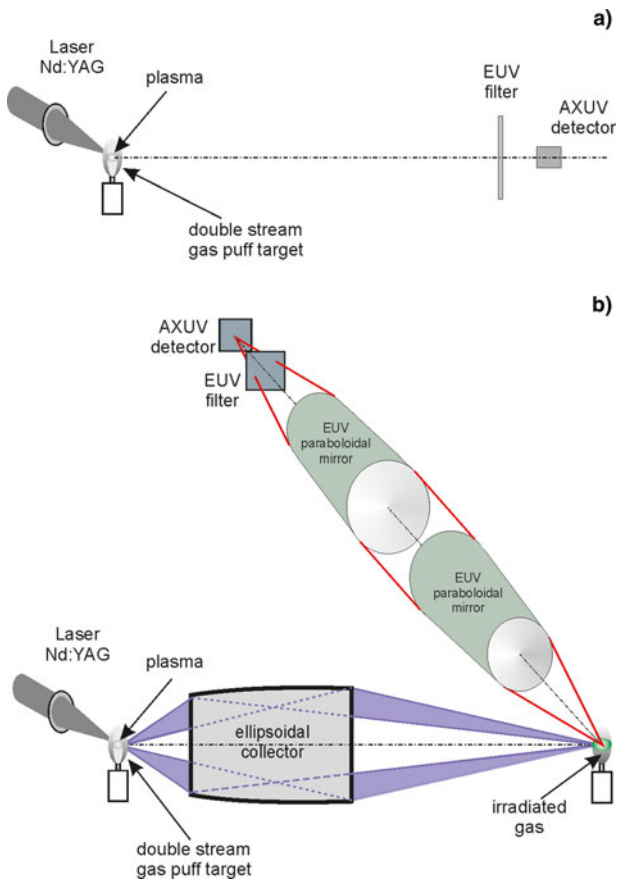


**Fig. 1.** Experimental arrangement: (a) a schematic view of the system for creation and detection of the SXR and EUV pulses emitted from the LPP source, (b) a schematic view of the system for creation of the EUV induced plasma and detection of EUV pulses emitted from such plasmas.

More detailed information concerning the double-stream gas-puff target and the LPP source can be found elsewhere Bartnik (2015).

### *EUV induced plasma*

The focused EUV beam was used for ionization of gases, injected into the interaction region, perpendicularly to an optical axis of the irradiation system, using an auxiliary gas-puff valve. The valve was equipped with a tube-shaped nozzle with an inner diameter of 2 mm. An outlet of the nozzle was located 2.5 mm from the optical axis of the EUV illumination system. The gas density, delivered to the interaction region, could be regulated within the range of approximately 1 ÷ 10% of the atmospheric density.

Irradiation of gases resulted in the formation of low-temperature plasmas, emitting radiation in a wide wavelength range, including the EUV range. Spectral measurements of this radiation were performed using an EUV spectrograph (McPherson, Model 251), equipped with a grazing incidence, flat-field toroidal grating, having a groove density of 450 gr/mm. Its spectral range was $\lambda \approx 10 \div 95$ nm and the spectral resolution for the wavelength of $\lambda = 50$ nm was approximately $\lambda/\Delta\lambda \approx 500$. The spectra were acquired using a back-illuminated charge-coupled device (CCD) detector (Princeton Instruments Inc.). To minimize a thermal noise the detector was cooled down to a temperature of −65 °C.

https://doi.org/10.1017/S0263034618000319 Published online by Cambridge University Press

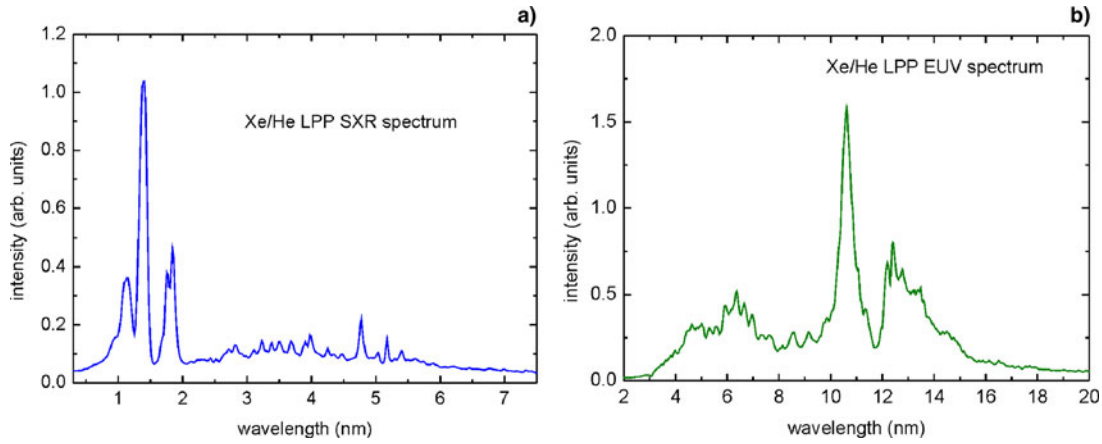


**Fig. 2.** Spectra corresponding to the LPP SXR (a) and EUV (b) sources driven by the Nd:YAG laser system (NL 129), working in the $\tau \approx 1$ ns (short pulse) and $\tau \approx 10$ ns (long pulse) regime, respectively.

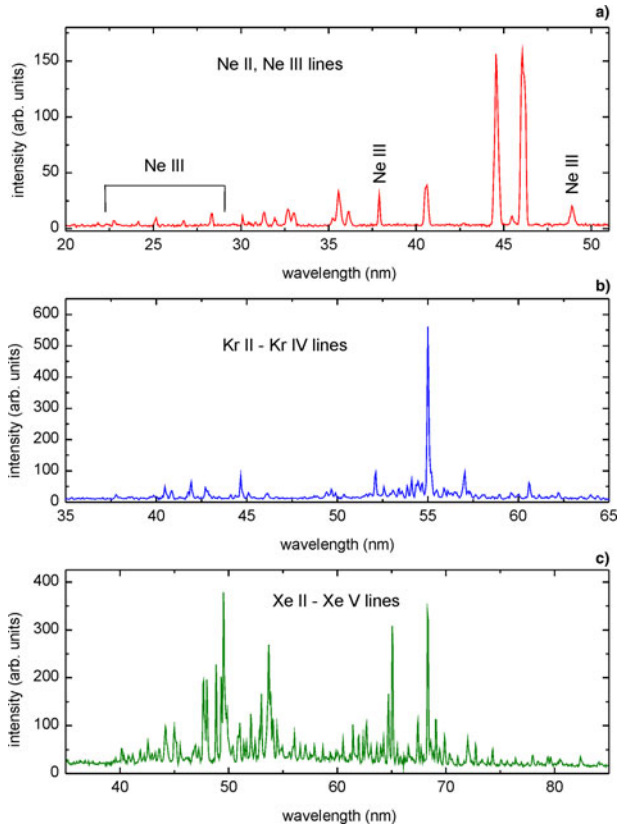


**Fig. 3.** EUV spectra, corresponding to low-temperature plasmas, induced in gases injected into the vacuum chamber, into the region of interaction with intense EUV pulses: (a) neon, (b) krypton, (c) xenon.

In this work, the EUV emission from plasmas induced in three rare gases: neon, krypton, and xenon was investigated. Spectra, recorded for these plasmas, are presented in Figure 3. The Ne spectrum consists of multiple lines, originating from transitions in singly and doubly charged ions. The most intense lines, at the wavelengths of 44.6 and 46.1 nm correspond to $2s^22p^5$-$2s2p^6$ and $2s^22p^5$-$2s^22p^4(^3P)3s$ transitions, respectively. The Kr and Xe spectra are composed of multiple lines originating from transitions in multicharged ions, Kr II – IV and Xe II – V, respectively. All these spectra are time integrated and were acquired by the accumulation of multiple spectral signals: 10 in case of Ne plasma, 200 in case of Kr and Xe plasmas. More details concerning formation and parameters of the EUV induced plasmas can be found elsewhere Bartnik *et al.* (2016), Bartnik *et al.* (2017).

It should be pointed out that relative intensities of these spectra, despite time integration and accumulation of multiple pulses, are very low. Acquisition of the spectra was possible due to a strong cooling of the CCD detector. It concerns especially Kr and Xe spectra, where cooling to a temperature −30 °C gave no spectra. In this case, only a thermal noise was obtained. This is the reason why a special detection system, containing an EUV collector, was prepared for the recording of time profiles of the EUV emission from photoionized plasmas.

The collector consists of two identical, axisymmetrical, paraboloidal mirrors, manufactured by RITE s.r.o., Czech Republic. Its collecting solid angle is about 0.05 sr. The EUV induced plasma was located in a focal position of the first mirror. This way a quasi-parallel EUV beam was formed. The second mirror was mounted such that the EUV beam, emerging from the first mirror, was focused at a distance of 260 mm from the plasma. To check the alignment of the paraboloidal system a back-illuminated CCD camera (DX420-BN, Andor) was used as a detector. For a selection of the spectral range of the EUV emission from Ne, Kr, and Xe photoionized plasmas, a 250 nm thick aluminum foil was employed. Additionally, a pinhole camera was used for imaging of the EUV induced plasma. The pinhole diameter had to be relatively large, equal to 0.2 mm, due to the weak EUV emission from the plasma. It was mounted at a distance of 90 mm from the plasma and a magnification of the camera was 0.8.

EUV induced plasma intensity distribution (a) and the focal plane intensity distribution of the paraboloidal collector (b), are shown in Figure 4. The FWHM of the image intensity distribution is approximately 1.5–2 mm. The plasma size is dependent on absorption properties of the gas used for the plasma production: the gas density and atomic scattering factors for a particular gas. The FWHM of the intensity distribution in the focal plane depends on plasma size and has the value of approximately 1.8–2.5 mm. A number of CCD counts, integrated over the area

https://doi.org/10.1017/S0263034618000319 Published online by Cambridge University Press

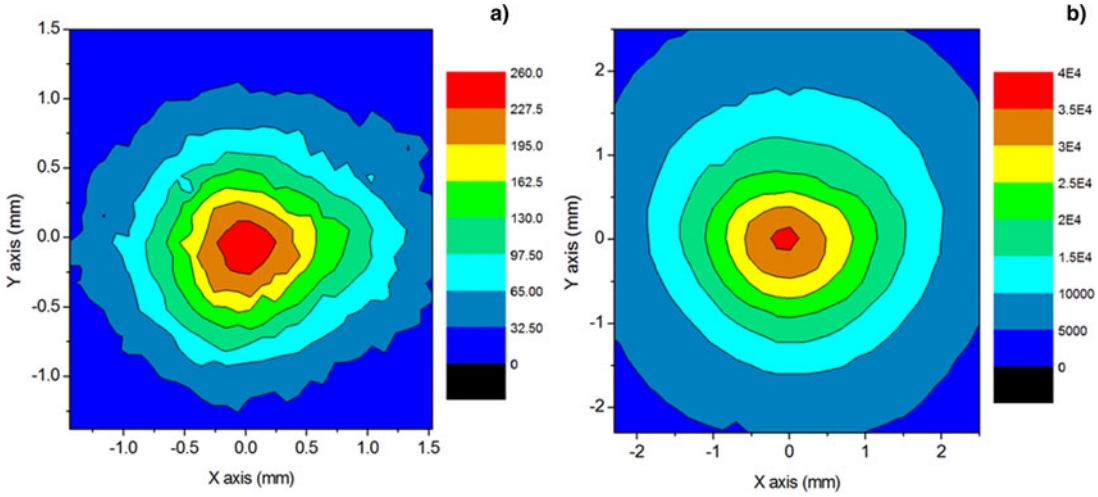


**Fig. 4.** Intensity distribution corresponding to: (a) the pinhole camera image of the EUV induced plasma, (b) image formed in the focal plane of the paraboloidal collector.

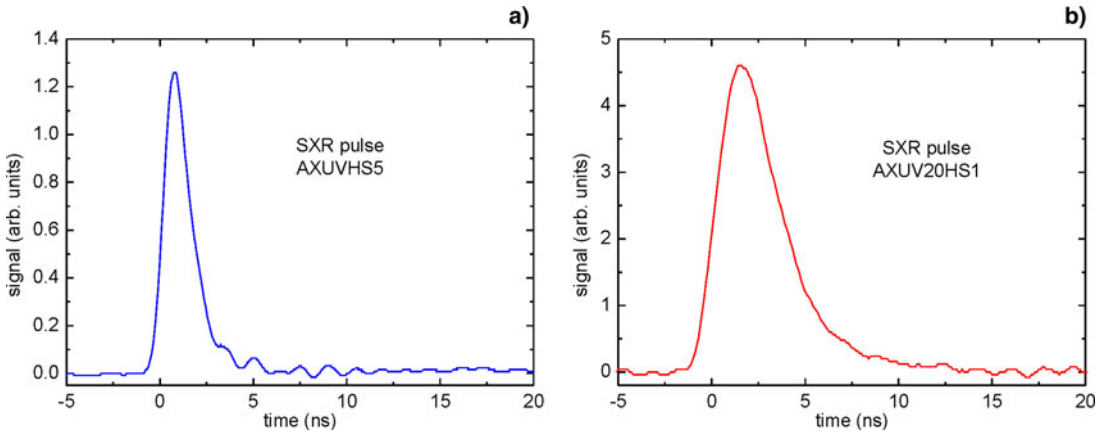


**Fig. 5.** Time profiles of signals, corresponding to the LPP SXR emission, recorded using AXUV detectors: (a) AXUVHS5, (b) AXUV20HS1.

shown in Figure 4b is approximately $4 \times 10^8$. In case of the Andor CCD camera, this value corresponds to $2.8 \times 10^9$ photoelectrons (gain – 7 photoelectrons per count), and approximately $3.7 \times 10^8$ photons with the wavelength of ~45 nm (the most intense Ne lines). Taking into account a quantum efficiency of the AXUV detectors, dedicated for the EUV radiation, QE ($\lambda =$ 45 nm) ≈5 it gives the number of electrons seen by the external circuit $\sim 2 \times 10^9$ ($Q \approx 3.2 \times 10^{-10}$ C). Assuming that the EUV emission time is comparable with the pulse width of the driving laser pulse, $\tau \sim 10$ ns, the expected amplitude of the generated voltage signal on the resistance $R = 50\ \Omega$ can be estimated to the value $R \times Q/\tau \approx 1.6$ V. It means that the number of photons in the focal spot of the paraboloidal collector should be sufficient for registration of the signal using an AXUV detector. The problem is that a fast detector AXUVHS1 Seely *et al.* (2002) has a very small active area of ~0.05 mm$^2$. It would give a very small signal, hardly distinguishable from the noise. The much better situation is in case of the AXUVHS5 detector with the active area of 1 mm$^2$ and the response time comparable with the HS1 detector. There is one more detector with a relatively short rise time <2 ns, namely AXUV20HS1. The active area of this detector is ~20 mm$^2$, which matches very well the focal spot area, shown in Figure 4b. These two detectors were used for measurements of the temporal profiles (traces) of the EUV emission from photoionized plasmas.

## Experimental results

The LPP SXR source utilizes the 1 ns regime of the laser operation, hence, the time duration of SXR pulses is of the same order. Using these pulses it was possible to compare response times of both detectors: AXUVHS5 and AXUV20HS1. A schematic view of the experimental set-up, employed for these measurements, is presented in Figure 1a. The detectors were reversely biased with a voltage of 100 V. For selection the SXR range and to decrease the radiation intensity, a 20 μm thick Al foil, acting as an absorption filter, was used. Typical signals, obtained for both detectors, are presented in Figure 5. It can be noticed that the signal recorded using the AXUVHS5 is much narrower compared with the signal obtained with the AXUV20HS1 detector. Pulse widths (full width half maximum (FWHM)) in both cases were ~1.8 and 3.8 ns, respectively. For comparison, the pulse profile was also measured using the AXUVHS1 detector. The profile was practically the same as measured using the AXUVHS5 detector. It means that for

https://doi.org/10.1017/S0263034618000319 Published online by Cambridge University Press

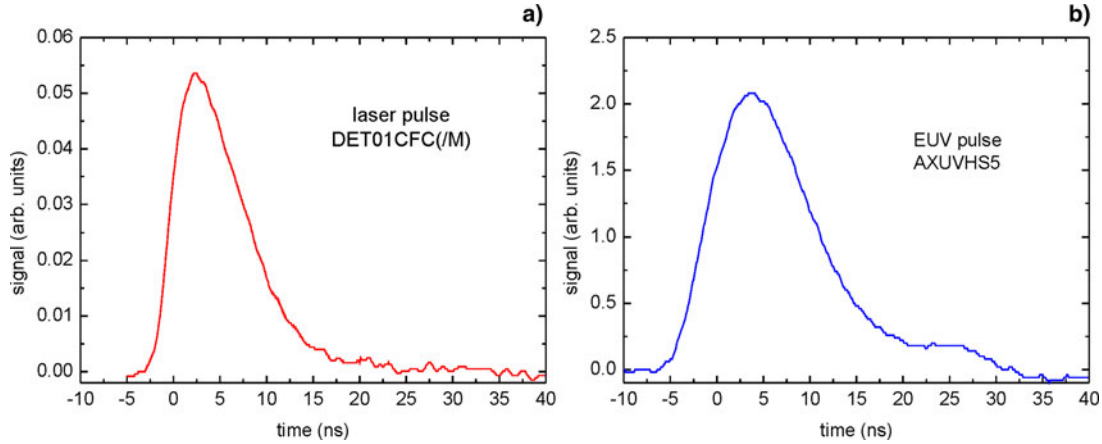


**Fig. 6.** Time profiles of signals, corresponding to the laser pulse of the NL 129 system, working in the long pulse regime (a) and the LPP EUV emission, recorded using the AXUVHS5 detector (b).

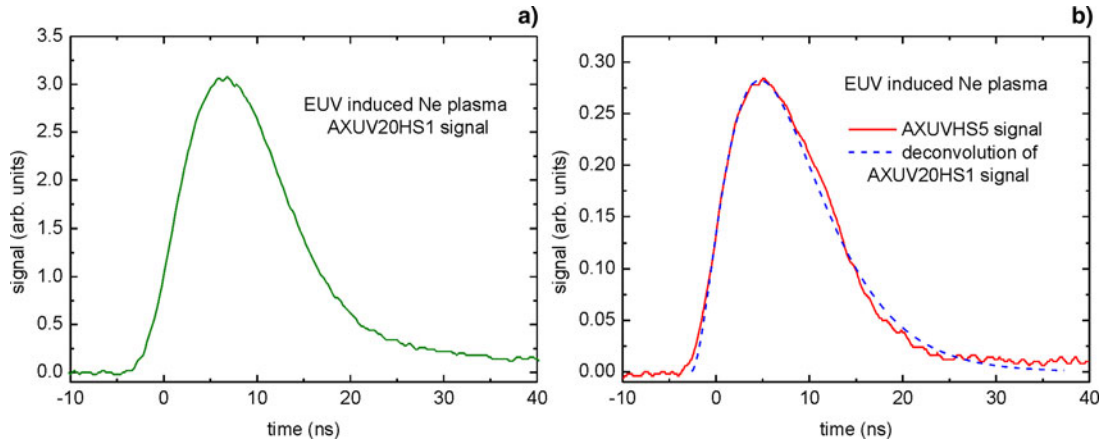


**Fig. 7.** Time profiles of signals, corresponding to the EUV emission from the EUV induced Ne plasma, recorded using AXUV detectors: (a) AXUV20HS1, (b) AXUVHS5.

measurements of the LPP SXR pulses, created using the NL-129 laser system, the AXUVHS5 can be employed while the response time of the AXUV20HS1 detector is too long. On the other hand, this time is much shorter compared with the EUV pulses emitted from the LPP or the EUV induced plasma.

Time profiles of the long laser pulse and the corresponding LPP EUV pulse are presented in Figure 6, respectively. The laser pulse (Fig. 6a) was measured using a fast photodiode DET01CFC(/M), Thorlabs, Inc. Its FWHM was approximately 8.7 ns, a little bit shorter compared with the nominal value. The corresponding EUV pulse, produced by the interaction of the laser pulse with the Xe/He gas-puff target, was measured using the AXUVHS5 detector. It can be noticed that the EUV pulse was longer compared with the laser pulse, its FWHM was 12.5 ns. It is connected with a fact that a plasma lifetime is usually longer in respect to the laser driving pulse. A typical emission in the visible wavelength range exceeds even 2 μs, as was shown in ref. Bartnik *et al.* (2018).

EUV induced plasmas were driven employing the LPP EUV pulses, hence, a time duration of the EUV emission from these plasmas was similar. It was expected that the response time of the AXUV20HS1 detector would be suitable for measurements of these pulses. Hence, the detector mounted in the focal area of the paraboloidal system was employed to measure time profiles of the EUV emission from plasmas induced in neon, krypton, and xenon gases. For a selection of an interesting spectral range, an absorption filter in a form of an aluminum foil, with a thickness of 250 nm, was used. Its transmission window corresponds to the emission spectra shown in Figure 3. The most intense emission was obtained for the Ne plasma. The signal amplitude was approximately 2 times larger compared with the value estimated in the previous section. In this case, a sufficiently high signal could be expected also from the AXUVHS5 detector. It was thus used to perform the comparative measurements of the signal profile. Both signals are presented in Figure 7. It can be noticed that they have similar shapes, however, the falling slope of the AXUV20HS1 signal is more smooth. The FWHM pulse widths of both signals are almost the same, 13.2 and 12.9 ns for the AXUV20HS1 and AXUVHS5 detector, respectively. Probably the most significant difference concerns the signal rise time, which in case of the AXUV20HS1 detector is approximately 1 ns longer.

Similar measurements were performed also for plasmas induced in Kr and Xe gases. From earlier measurements of the focal spot, performed using the CCD camera, and the spectral measurements it was clear that signals with a few times smaller amplitudes should be expected. In fact, amplitudes of signals obtained using the AXUV20HS1 detector, presented in Figure 8a were approximately 5 and 6 times smaller for Xe and

https://doi.org/10.1017/S0263034618000319 Published online by Cambridge University Press

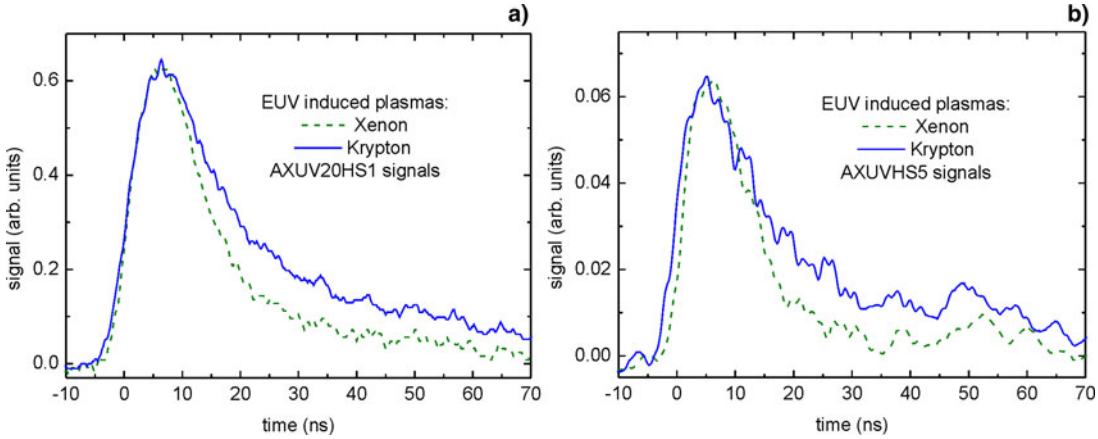


**Fig. 8.** Time profiles of signals, corresponding to the EUV emission from the EUV induced Xe and Kr plasmas, recorded using AXUV detectors: (a) AXUV20HS1, (b) AXUVHS5.

Kr plasmas, respectively. Also, time profiles of these signals were significantly different compared with the Ne plasma. In the case of the Xe plasma, the signal rise time was 5.8 ns (5.6 ns for Ne plasma) and its pulse width (FWHM) was 14.6 ns. These values were visibly longer compared with the corresponding signal from Ne plasma, however, not as long as for the Kr plasma. In this case, the rise time was 6.6 ns and the FWHM 18.6 ns. For comparison, these measurements were performed using the AXUVHS5 detector. Typical time profiles of the recorded signals are presented in Figure 8b. As could be expected, their amplitudes are of order of magnitude lower and they are much more noisier compared with signals obtained using the AXUV20HS1 detector. Their rise times are also a little bit shorter (approximately 1 ns) compared with the AXUV20HS1 signals. These measurements also indicate that the pulse widths are larger compared with the Ne pulse and that the Kr emission pulse is longer compared with the Xe pulse.

## Discussion of the results

In this work the detection system consisted of the paraboloidal, EUV collecting system and the AXUV20HS1 detector, was tested concerning its applicability to measure time profiles of EUV pulses, emitted from EUV induced plasmas. Time profiles obtained using this detector were compared with the corresponding profiles recorded using the AXUVHS5 detector having a rise time below 1 ns. The comparison performed for the LPP SXR source, driven by the short laser pulse, where a time duration of the SXR pulse is of the order of 1 ns, indicates that the response time of the AXUV20HS1 detector is too long. The pulse width of the AXUV20HS1 signal was approximately two times longer compared with the AXUVHS5 pulse. It means that the AXUV20HS1 cannot be used for measurements of such short pulses. On the other hand, the LPP EUV source is driven by laser pulses even of order of magnitude longer. In this case, the time duration of the EUV pulse is also much longer. The FWHM of EUV pulses, measured for laser-produced Xe plasmas, driven by laser pulses with the time duration of approximately 8.7 ns, was 12.5 ns (see Fig. 6). The EUV emission from EUV-induced plasmas should have a similar time duration. In fact, the emission time was even longer. The comparative measurements performed for the EUV-induced Ne plasmas, using both detectors, indicated that differences in time profiles are not very significant. It means, that in case of lack of some fine structure of the EUV pulse in the ns or sub-ns scale the AXUV20HS1 detector can be used. A possibility to use the AXUV20HS1 detector is especially important in case of detection of much weaker signals, of order of magnitude lower, or even more. It can be noticed that amplitudes of signals recorded for EUV-induced Xe and Kr plasmas, are approximately 5 times lower compared with the corresponding signal obtained for Ne plasmas and their quality is good. On the other hand, amplitudes of these signals measured using the AXUVHS5 detector are of order of magnitude smaller, and they are deformed significantly by an electrical noise. Using the AXUV20HS1 detector, in this case, is thus a good option.

The detection system, equipped with the paraboloidal collector, employed in this experiment, allows detecting the EUV radiation in a wide wavelength range. The system, however, after some modifications can be used for measurements of signals corresponding to individual spectral lines. It can be done employing an additional flat multilayer mirror mounted between paraboloidal mirrors in off-axis configuration. In this case, a parallel beam formed by the first paraboloidal mirror would be reflected under a Bragg angle from the flat multilayer mirror and focused by the second paraboloidal mirror. The reflection angle can be adjusted to select a single or multiple spectral lines. Taking into account that even in case of selection of the most intense lines from spectra presented in Figure 3, the corresponding EUV signal can be of order of magnitude lower compared with the signal spanning the entire EUV spectrum. In case of the Xe or Kr plasma emission, the signal amplitude using the AXUVHS5 detector would be comparable with the noise. In this case, the AXUV20HS1 detector could give a reasonable signal.

In principle, it can be assumed that the AXUV20HS1 signal corresponding to the SXR pulse (Fig. 5b) represents its response for a Dirac delta function. In this case, it can be used for deconvolution of the EUV signals recorded using this detector. Such deconvolution was performed for the signal shown in Figure 7a corresponding to Ne plasma emission. The resulting profile is presented in Figure 7b, together with the signal obtained using the AXUVHS5 detector. The agreement of both profiles is very good, the rise times and the pulse widths are almost the same. A small difference concerns the falling slope, which in case of the deconvoluted AXUV20HS1 signal is smoother, while the AXUVHS5 signal has a small, however, clearly visible “hump”.

https://doi.org/10.1017/S0263034618000319 Published online by Cambridge University Press

Results of temporal measurements indicate that the time of the EUV emission from EUV induced plasmas more or less corresponds to the irradiation time. This time is only a little bit longer in case of Ne plasmas (below 1 ns) and Xe plasmas (~2 ns). The more pronounced difference was observed in case of Kr plasmas, where the FWHM value exceeded 18 ns, which means that the pulse width was approximately 6 ns longer compared with the driving EUV pulse. An origin of these differences is not clear and requires further investigation. Longer emission time compared with the driving pulse means that a part of energy delivered as EUV photons was stored in excited states with relaxation times exceeding 10 ns or in the electron gas, cooled down slowly due to a sufficiently long average time between inelastic collisions with ions. In principle, both mechanisms are possible taking into account a relatively low electron density and a variety of relaxation times of excited states, mainly in the nanosecond scale. Temporal measurements, performed for individual lines, should help to clarify this issue. It could be done using the flat multilayer mirror, as mentioned above, for the line selection.

## Summary

In this paper, the detection system, developed for temporal measurements of weak EUV signals propagating in a vacuum chamber under the pressure of the order of 0.1–0.01 mbar, is presented. The system is based on the paraboloidal collector and semiconductor detectors sensitive for the EUV photons. The collector allows focusing a part of the radiation emitted from a point-like source onto the detector surface. Additional absorption filter allows for selection of an interesting wavelength range. The system was used for measurements of the EUV radiation signals emitted from low temperature, EUV induced plasmas, having the size of the order of 1 mm. Plasmas were created by irradiation of small portions of gases, injected into the vacuum chamber, using the LPP EUV source. Three gases were used for the EUV induced plasma formation: neon, krypton, and xenon. Plasmas, created in these gases, emitted radiation in similar wavelength ranges, spanned by the transmission range of the Al 250 nm absorption filter, used for spectral selection of the detected radiation pulses. Two detectors, AXUV20HS1 and AXUVHS5, having different response times and active areas, were used for the measurements. It was shown, that in case of EUV pulses with the FWHM exceeding 10 ns, differences between the profiles of the corresponding signals, obtained using both detectors, were not very significant. On the other hand, the amplitude of the signal recorded by the AXUV20HS1 detector is an order of magnitude higher. It was, thus concluded, that to detect very weak EUV signals with the pulse duration of the order of 10 ns, the AXUV20HS1 detector would be a good compromise. Using both detectors, it was also demonstrated that the EUV emission times from plasmas created in different gases are comparable with the driving EUV pulse. The shortest time of the EUV emission was observed for Ne plasmas. The corresponding pulse width was only a few hundred ps longer in respect to the driving EUV pulse. The longest time was observed for Kr plasmas, approximately 1.5 times the FWHM of the driving pulse.

**Acknowledgements.** This work was supported by the National Science Centre, Poland, grant agreement no. UMO-2016/21/B/ST7/02225, and partially by European Union's Horizon 2020 Programme (LASERLAB-EUROPE) grant agreement no. 654148.

## References

**Abrikosov A, Reshetnyak V, Astakhov D, Dolgov A, Yakushev O, Lopaev D and Krivtsun V** (2017) Numerical simulations based on probe measurements in EUV-induced hydrogen plasma. *Plasma Sources Science and Technology* **26**, 045011.

**Bartnik A** (2015) Laser-plasma extreme ultraviolet and soft X-ray sources based on a double stream gas puff target: interaction of the radiation pulses with matter (Review). *Optoelectronics Review* **23**, 172–186.

**Bartnik A, Fiedorowicz H, Jarocki R, Kostecki J, Rakowski R and Szczurek M** (2008) EUV emission from solids illuminated with a laser-plasma EUV source. *Applied Physics B: Photophysics and Laser Chemistry* **93**, 737.

**Bartnik A, Pisarczyk T, Wachulak P, Chodukowski T, Fok T, Wegrzynski L, Kalinowska Z, Fiedorowicz H, Jarocki R, Szczurek M, Krousky E, Pfeifer M, Skala J, Ullschmied J, Dostal J, Dudzak R, Hrebícek J, Medrik T, Cikhardt J, Cikhardtova B, Klir D, Rezac K and Pina L** (2015) Photoionized plasmas in laboratory: a connection to astrophysics and planetary sciences. *Proc. of SPIE 9510, EUV and X-ray Optics: Synergy between Laboratory and Space IV, 95100P.*

**Bartnik A, Wachulak P, Fiedorowicz H and Skrzeczanowski W** (2016) Kr photoionized plasma induced by intense EUV pulses. *Physics of Plasmas* **23**, 043512.

**Bartnik A, Skrzeczanowski W, Wachulak P, Saber I, Fiedorowicz H, Fok T and Węgrzyński L** (2017) Low-temperature photoionized plasmas induced in Xe gas using an EUV source driven by nanosecond laser pulses. *Laser and Particle Beams* **35**, 42–47.

**Bartnik A, Skrzeczanowski W, Fiedorowicz H, Wachulak P and Fok T** (2018) Low-temperature plasmas induced in nitrogen by extreme ultraviolet (EUV) pulses. *Laser and Particle Beams* **36**, 76–83.

**Chalupský J, Boháček P, Burian T, Hájková V, Hau-Riege SP, Heimann PA, Juha L, Messerschmidt M, Moeller SP, Nagler B, Rowen M, Schlotter WF, Swiggers ML, Turner JJ and Krzywinski J** (2015) Imprinting a Focused X-Ray Laser Beam to Measure Its Full Spatial Characteristics. *Physical Review Applied* **4**, 014004.

**Gerasimova N, Dziarzhytski S, Weigelt H, Chalupský J, Hájková V, Vyšín L and Juha L** (2013) *In situ* focus characterization by ablation technique to enable optics alignment at an XUV FEL source. *Review of Scientific Instruments* **84**, 065104.

**Huang Z** (2013) Brightness and coherence of synchrotron radiation and fels. *Proceedings of the 4th International Particle Accelerator Conference, 16–20.* Zhimin Dai, Christine Petit-Jean-Genaz, Volker R.W. Schaa, Chuang Zhang, Editors.

**Könneckea R, Follath R, Pontius N, Schlappa J, Eggenstein F, Zeschke T, Bischoff P, Schmidt J-S, Nolla T, Trabanta C, Schreck S, Wernet Ph, Eisebitt S, Senf F, Schüßler-Langeheine C, Erko A and Föhlisch A** (2013) The confocal plane grating spectrometer at BESSY II. *Journal of Electron Spectroscopy and Related Phenomena* **188**, 133–139.

**Seely JF, Boyer CN, Holland GE and Weaver JL** (2002) X-ray absolute calibration of the time response of a silicon photodiode. *Applied Optics* **41**, 5209–5217.

**van der Horst RM, Beckers J, Osorio EA, Astakhov DI, Goedheer WJ, Lee CJ, Ivanov VV, Krivtsum VM, Koshelev KN, Lopaev DV, Bijkerk F and Banine VY** (2016) Exploring the electron density in plasma induced by EUV radiation: I. Experimental study in hydrogen. *Journal of Physics D: Applied Physics* **49**, 145203.

https://doi.org/10.1017/S0263034618000319 Published online by Cambridge University Press